# Studying diffusion of a cloud emitted by a pulsed source in the turbulent atmosphere

## Yu.S. Balin, A.D. Ershov, A.I. Bril,[1] V.P. Kabashnikov,[1] V.M. Popov,[1] and A.P. Chaikovskii[1]

*Institute of Atmospheric Optics,*
*Siberian Branch of the Russian Academy of Sciences, Tomsk, Russia*
*[1] Institute of Physics,*
*Belarus National Academy of Sciences, Minsk, Belarus*

Diffusion of a cloud emitted by a pulsed source was studied in field and numerical experiments. The field experiment was conducted in summer in steppe with the use of remote and local monitoring instrumentation. A source emitting the cloud was modeled by a charge with an indicator substance set off at the height of 10 m. The cloud formed of the condensed-phase products of explosion was monitored with a scanning lidar. The ratio of the backscattering signal from the cloud to the signal from the background aerosol, as well as the time and coordinates of sensing points, was recorded. At the distance of 25\$30 m from the site of explosion, an ultrasonic meteorological station measured the air temperature, vertical and horizontal components of the wind speed and its direction, total energy of turbulent motions, the level of tangential turbulent friction stress, and vertical turbulent heat flux. The experimental lidar data were compared with the results of numerical simulation of the spatial distribution of the pollutant using the statistic Gaussian distribution model. The calculated results as a whole are in a close agreement with the experiment.

## Introduction

Diffusion of emissions from continuous or pulsed sources depends on numerous related factors: physical or chemical nature of a substance, meteorological situation (temperature and wind stratification of the atmosphere), the height of the source with respect to obstacles to motion of the air flow, local topography, etc.).

At atmospheric monitoring connected with estimation of the quality of air basin, emissions are usually monitored with stationary or mobile ground-based tools. Unfortunately, these tools do not provide for the needed spatial and temporal resolution, especially as only the surface atmospheric layer is monitored.

The situation is aggravated if it is necessary to monitor consequences of the effect of technogenic pollutants on the environment in the atmospheric boundary layer in the case of explosions, spraying of various substances from airplanes, emergencies at large industrial plants, etc. Rising in the atmosphere up to the altitudes of 0.3\$1 km, an aerosol-gas cloud transforms due atmospheric turbulence and moves with the wind from the source, settling on the ground. Cloud diffusion often has a random character, therefore it seems problematic to prearrange the needed number of ground-based monitoring sites along the cloud path.

Most acceptable monitoring tools in this situation are those based on remote methods for determination of pollution parameters (active and passive sensing) that provide for the possibility of obtaining the needed information in real time and on large spatial scales. With the use of passive sensing methods, atmospheric diffusion of pollutants from an instantaneous source was studied in many papers.[1$4,6] However, these methods give only an instantaneous image of a cloud in only one plane, thus given the two-dimensional distribution of the pollutant concentration over the objective's field of view.

Active sensing, in particular, with a scanning lidar eliminates this disadvantage giving the 3D distribution of a pollutant, i.e., determines the object's structure both in the external boundaries and in depth. Besides, a lidar can monitor a cloud even in such cases that it is invisible visually or by a photo camera, for example, at night, low concentration of the pollutant, or low contrast of the cloud against the background of the environment. An example of such application of a lidar to sensing of aerosol emitted at explosion was demonstrated by Collis as early as in 1968 (see Ref. 5). Nevertheless, publications about the use of lidars to study pollution diffusion in the atmospheric boundary layer are still few. This paper describes the results of field measurements of the dynamics of diffusion of an explosion product cloud and compares them with the calculated data.

## Description of the experiment

Field experiments on studying the processes of pollution diffusion were conducted in June 1999 in steppe

under the conditions of stable anticyclone. These conditions were characterized by fine cloudless weather and stable diurnal dynamics of meteorological and turbulent parameters of the atmosphere. In this paper, we present one of typical experiments conducted on June 8 at 17:37 LT.

The measuring system included the equipment for remote sensing and the BMK-01 ultrasonic meteorological station, which measured meteorological and turbulent parameters of the atmosphere in a local volume of the atmospheric surface layer.

A lidar was located 770 m far from an explosion mast in the back sector from the excepted direction of spread of the explosion products. A charge (10 kg of TNT equivalent) set off at the height of 10 m served a source of an indicator substance, which allowed the explosion products to be selected from the natural aerosol based on the cloud tracks on the ground. The experiment involved the LOZA-M small-sized scanning single-frequency lidar sensing the atmosphere at the wavelength of 532 nm with the spatial resolution of 7.5 m and the angular resolution of 10 arc min. The energy per pulse was 25 mJ with the pulse repetition frequency of 5 Hz. The sensing range was about 3 km.

The cloud of the condensed-phase explosion products was tracked for 6 min. For this time, the cloud moved about 2 km away from the place of explosion and achieved the height of more than 200 m.

One of the tasks of the lidar observations was to obtain spatial cross sections of a cloud in the horizontal and vertical planes. This allows the space-time pattern of cloud spread to be represented fragmentally and as a whole and, with the estimated speed and direction of the cloud drift, the angular extension of the cloud to be determined at all stages of its transformation, the projection of the cloud track onto the ground to be found, etc. Another task was to determine the inner cloud structure at different time in the process of moving away from the point of explosion. Omitting methodic details connected with the problem of inversion of the sensing data for optical parameters and then the mass concentration of aerosol (this problem is considered in sufficient detail in Refs. 12 and 13), note only that in this case the consideration can be restricted to the information about the amplitude ratio of lidar signals from the background atmosphere and the atmosphere disturbed by the explosion products.

Before the beginning of the experiment, the lidar conducted sensing in the forward hemisphere to determine the background optical parameters of the atmosphere in the selected sectors. Then, starting from the time of explosion, scanning by sensing pulses in the horizontal plane was conducted with neighboring directions separated by the angle of 0.1$0.5°. Scanning was continued as long as the echo signal from the cloud was observed. Then the lidar changed the sensing direction in the vertical plane by 0.5$1° and again performed horizontal scanning of the atmosphere in the back

direction. At every laser shot, the information on the direction of sensing, digitized amplitude of lidar signals, and the current time came from elevation and azimuth sensors of a turning column to the computer memory. Thus, the spatial mapping of the cloud resulted from the sequential accumulation of azimuth cross sections at different angles of elevation.

Since the object of study was a nonstationary formation of aerosol particles from a pulsed source, knowing the distance passed by the cloud and the time of observation, the vertical and horizontal components of the drift speed and the direction of the aerosol cloud can be estimated.

The BMK-1 ultrasonic meteorological station[14] was spaced by 25$30 m from the place of explosion. It measured the mean and instantaneous values of the air temperature, vertical and horizontal components of the wind speed and its direction at the height of 2.5 m. This allowed determination of the total energy of turbulent motions, the tangent turbulent friction stress, the vertical turbulent heat flux, the Monin# Obukhov scale, the structure functions of temperature and speed fluctuations, and the coefficients of turbulent heat and momentum exchange.

## Mathematical model

For mathematical simulation of cloud spread, we used the Gauss statistical model,[6,7] according to which the average (over the ensemble) concentration $c$ in the instantly arising aerosol cloud can be estimated by the following equation:

$$c(x, y, z) = \frac{Q}{(2\pi)^{3/2} S_x(t) S_y(t) S_z(t)} \times$$

$$\times \exp\left[-\frac{x^2}{2S_x^2(t)} - \frac{y^2}{2S_y^2(t)} - \frac{z^2}{2S_z^2(t)}\right], \qquad (1)$$

where $x$, $y$, and $z$ are the coordinates measured from the cloud center of gravity; $S_x(t)$, $S_y(t)$, and $S_z(t)$ are the cloud root-mean-square dimensions depending on the time $t$ from the emission; $Q$ is the total mass of the emitted substance.

The most time the cloud moved far above the surface layer (its altitude can be estimated, for example, from Ref. 10) in the region of quasi-homogeneous turbulence, where the vertical dimension of the cloud can be estimated by the equation[6$9]

$$S_z^2(t) = S_z^2(0) + \Delta S_n^2(t_k) +$$

$$+ 0.5 \, D_v^E(\delta_k)(\tau_L^W)^2 \, [1 - \exp(-\eta)]^2 +$$

$$+ 2(w\tau_L^W)^2 [\eta - 1.5 - 0.5\exp(-2\eta) + 2\exp(-\eta)], \quad (2)$$

where $t_k$ is the time at which the cloud leaves the surface layer; $D_v^E(\delta_k)$ is the Euler structure function of speed, $\delta_k = S_z(t)$; $\tau_L^W$ is the Lagrange correlation time of the vertical velocity component of a liquid particle; $w$ is the root-mean-square value of turbulent pulsations of the velocity component;

$$\eta = (t \$ t_k) / \tau_L^W. \qquad (3)$$

The cloud dimensions in the horizontal plane can be determined by the equations similar to Eq. (2).

Since an actual device cannot measure the concentration not exceeding some value $c_{min}$, the observed cloud dimensions and the total mass of the emitted substance differ from the actual ones. The observed cloud mass can be found through integration of the concentration over the area bounded by the condition $c \geq c_{min}$. The square of observed characteristic dimension of the cloud can be determined as an integral of the concentration multiplied by the square coordinate over the area defined above divided by the observed mass. Within the framework of the Gauss statistical model, the observed cloud mass $M$ is determined by the equation

$$M = Qm, \qquad (4)$$

where

$$m = \int_0^g \exp(-\xi) \, \text{erf}(\sqrt{g-\xi}) \, d\xi, \qquad (5)$$

$$g = \ln [Q/ c_{min} (2\pi)^{3/2} S_x S_y S_z]. \qquad (6)$$

The observed root-mean-square dimensions of the cloud are

$$R_i = S_i \sqrt{1 - f/m}, \qquad (7)$$

where $i$ is for $x$, $y$, and $z$;

$$f = 4(3\sqrt{\pi})^{-1} g^{3/2} \exp(-g). \qquad (8)$$

As the cloud dimensions increase, the value of the parameter $g$, depending on the ratio of the concentration at the center of the cloud to the minimal detectable concentration, decreases. As this proceeds, the observed cloud dimensions $R_i$ and mass $m$ increasingly differ from the actual ones. At $g$ equal to zero the cloud becomes invisible.

## Comparison of experimental and calculated data

Experimental data are presented by the array of concentrations supplemented with the values of three spatial coordinates and time. One of the peculiarities of lidar sensing is that different areas of space are sensed at different time. To draw the complete spatial pattern, one should take data from some finite time interval $T$. This may cause errors connected both with non-stationarity of the object and with the insufficient length of this interval.

Let us estimate the errors arising when assessing the cloud dimensions from the sensing data using, as an example, the Gauss statistical model, assuming that the lidar can record arbitrarily small concentration. We consider the time-periodic sensing scheme, whose single cycle consists in discrete exhaustion of angles of elevation within the limits exceeding the vertical angular dimension of the cloud.

It is assumed that a series of measurements with different azimuth angles, whose range covers the horizontal angular cloud dimension, is conducted at every value of the angle of elevation. Every shot in the object's plane can be put in correspondence with an elementary area $\Delta y \Delta z$, through whose center the sensing pulse passes, equal to the angular steps multiplied by the distance to the object.

Let us try to estimate the cloud dimension by the equation

$$\overline{x_i^2} = \frac{1}{M_{exp} T} \int dx \, dy \, dz \, x_i^2 \int_{t-T/2}^{t+T/2} d\tau \, c_{exp}(x,y,z,\tau), \qquad (9)$$

where

$$M_{exp} = \frac{1}{T} \int dx \, dy \, dz \int_{t-T/2}^{t+T/2} d\tau \, c_{exp}(x,y,z,\tau); \qquad (10)$$

$T$ is the time of experimental data averaging; the axis $x$ coincides with the direction to the cloud; $c_{exp}$ is the experimentally measured concentration. Within the framework of the Gauss model and the accepted sensing scheme for the cloud moving with the speed $U$ along the axis $x$, we have

$$c_{exp}(x,y,z,t) = \sum_k \delta(t-t_k) \, Q \left[(2\pi)^{1/2} R_x\right]^{-1} \times$$

$$\times \exp \{\$ (x_j \$ Ut)^2 / 2R_x^2\} f_{yz}(k), \qquad (11)$$

where $k$ numbers sensing pulses; $x_j$ is the central coordinate of the interval containing $x$. The length of this interval $\Delta x$ is equal to the spatial resolution along the direction of sensing:

$$f_{yz}(k) = \begin{cases} \left[(2\pi) \, R_y R_z\right]^{-1} \exp\{- y_k^2 / 2R_y^2 - z_k^2 / 2R_z^2\} \\ 0 \end{cases}, \qquad (12)$$

$f_{yz}(k)$ is nonzero and takes the value given in the upper line only if $y$ and $z$ fall within the area associated with the $k$th shot. Equation (11) simulates lidar experimental data and accounts for the above peculiarity of lidar sensing that at every instant we have the data for only one point of the pattern plane and the data for another point of the pattern plane correspond to different time.

For simplicity, let us assume that the integration steps $\Delta x$, $\Delta y$, and $\Delta z$ are constant, and the cloud dimensions do not change with time. Substituting Eq. (11) into Eq. (9) and changing the order of integration with respect to the spatial variables and time, we obtain

$$M_{\exp} = Q \sum_{k=k1}^{k2} \left[(2\pi)\, R_y R_z\right]^{-1} \times$$

$$\times \exp\{\$\, y_k^2 / 2R_y^2\, \$\, z_k^2 / 2R_z^2\}\, \Delta y\, \Delta z; \qquad (13)$$

$$\overline{x^2} = R_x^2 , \qquad (14)$$

$$\overline{y^2} = \frac{Q}{M_{\exp}} \sum_{k=k1}^{k2} \left[(2\pi)\, R_y R_z\right]^{-1} y_k^2 \times$$

$$\times \exp\{\$\, y_k^2 / 2R_y^2\, \$\, z_k^2 / 2R_z^2\}\, \Delta y\, \Delta z, \qquad (15)$$

where $k1$ and $k2$ are the numbers of the pulses corresponding to the time boundaries of the averaging interval. The equation for $\overline{z^2}$ is similar to Eq. (15).

According to Eq. (14), the longitudinal dimension can be reconstructed exactly from the data for any one shot in the area with substance concentrations far exceeding the minimal detectable one. It can be seen from Eq. (15) that the values of $\overline{y^2}$ and $\overline{z^2}$ depend on the current time and the interval $T$ through the time dependence of the boundary pulse numbers $k1$ and $k2$.

Numerical estimates were made for the rectangular $5R_y \times 5R_z$ scanning area in the plane $(yz)$. The cloud was at the center of this area, $\Delta y = 0.5R_y$, $\Delta z = 0.5R_z$. All the times were related to the time of one scan of the studied area (the time of a single scanning cycle), and the reconstructed dimensions were related to their œtrueB rms values. It can be seen from Fig. 1 that to estimate the horizontal dimension, we need the data from the time interval $T$ on the same order of magnitude as or longer than the time of one horizontal scan, and to estimate the vertical dimension, we need the data from the time interval $T$ on the same order of magnitude as or

longer than the time of a single cycle. In this example, the former is ten times shorter than the latter.
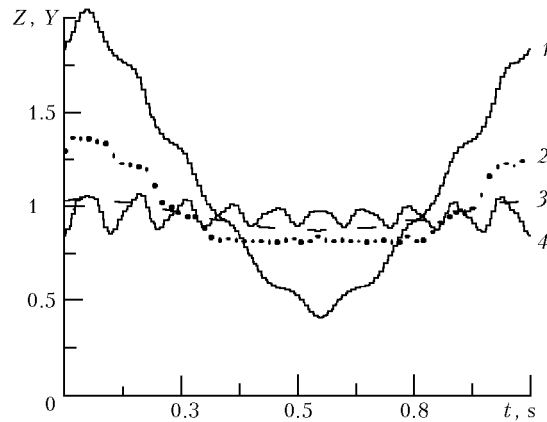


**Fig. 1.** Ratio of the dimensions reconstructed from the data modeling the experiment to the œtrueB dimensions as a function of time related to the time of one scan of the field of view: vertical (*1*$*3*) and horizontal (*4*) dimension; $T = 0.33$ (*1*, *4*), 0.7 (*2*), and 2.5 s (*3*).

In the considered experiment, the time of one scan increased with time roughly from 0.5 to 1 min. According to this, when comparing with the calculated data, the averaging interval for the experimental data was taken equal to $T = 30 + 0.1t$. It is undesirable to take a long averaging interval, as for the time $T$ the cloud may markedly change its dimensions. To obtain the statistical characteristics of the cloud for the fixed time $t$, we took all concentrations measured in the finite time interval from $t\, \$\, T/2$ to $t + T/2$ and the corresponding coordinates. Then the space area containing all the coordinates was divided into elementary rectangular parallelepipeds, containing many points, on the average. To calculate the integrals, the function values averaged within every parallelepiped and multiplied by its volume were summed over all parallelepipeds. Thus, coordinates of the cloud center of gravity and its rms dimensions along the mean wind $R_x^2$ and across the wind $R_y^2$, as well as the vertical dimension $R_z^2$ were determined. The spatial domain of integration was divided into 27, 125, and 1000 elementary parallelepipeds.

The general idea on the cloud geometry can be gained from Fig. 2, which shows the coordinates $(x, y)$ and $(x, z)$ of sensing points during the experiment. Every track consisting of points along the segment of the straight line corresponds to one shot. Solid curves in Fig. 2 are projections of the trajectory of the cloud center of gravity onto the horizontal and vertical planes as calculated from the experimental data.
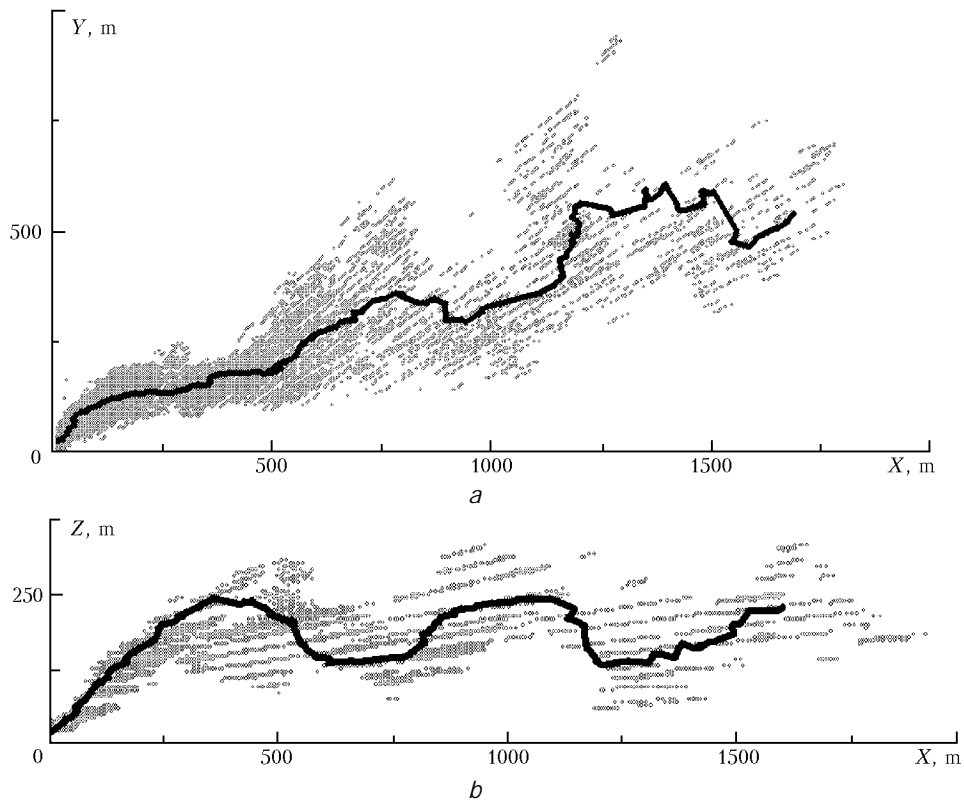
**Fig. 2.** Projections of all sensing points onto the horizontal (*a*) and vertical (*b*) planes. The trajectory of the cloud center of gravity calculated based on the experimental data is shown as a solid curve.

As initial data in calculations, we used the experimentally measured air temperature of 29°C, wind velocity of 4 m/s at the height of 2.5 m, friction velocity $u_* = 0.2$ m/s, and the Obukhov scale $L = \$ 6.2$ m. To calculate the Lagrange correlation time of velocity components, the height of the mixing layer was first estimated by the equation $H_m = Z_m 0.4\, u_*/f_{Cor}$ (Ref. 11), where $f_{Cor}$ is the Coriolis parameter; $Z_m$ is the dimensionless coefficient. For the conditions of summer and unstable atmospheric stratification, $Z_m = 0.7$ (Ref. 11). Then the velocity scale under the convective conditions $w_* = u_* (2.5 H_m/|L|)^{1/3}$ was calculated, as well as the variance of turbulent pulsations of the velocity. The latter and the Lagrange correlation time of the velocity components in the unstably stratified atmospheric boundary layer were calculated by the approximating equations given in Ref. 7. The calculated energy of turbulent pulsations averaged over the mixing layer (1.5 m²/s²) turned out to be very close to the data of measurements at the height of 2.5 m.

Figure 3 depicts the time dependence of the observed dimensionless cloud mass and radius as calculated by Eqs. (5) and (7). The unknown parameter $Q/c_{min}$ was fitted from the condition $g = 0$ at the limit sensing range, which was equal to 3 km in our experiment. This separation of the cloud from the lidar was observed roughly 400 s after the explosion. Further calculations were performed with $Q/c_{min}$ determined just in this way.
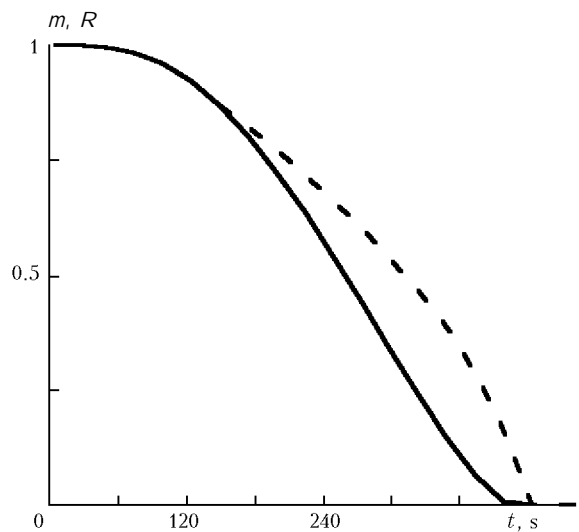


**Fig. 3.** Observed dimensionless cloud mass (solid curve) and dimension (dashed curve) as calculated by Eqs. (5) and (7).

Figures 4$6 depict the longitudinal, cross, and vertical dimensions of the cloud obtained from processing of the lidar data and calculated by Eqs. (5) and (12). Smooth curves correspond to the calculation. Irregular curves were obtained from the experimental data through numerical integration as described above at different spatial fragmentation.
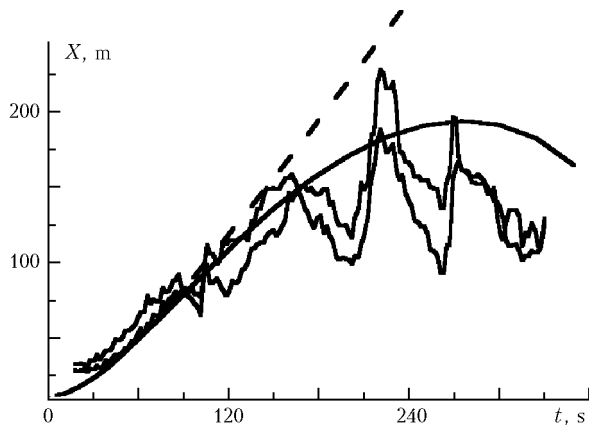
**Fig. 4.** Time dependence of the longitudinal cloud dimension: result of experimental data processing at division of the integration domain into 27 and 1000 parts (irregular curves), calculation by Eq. (2) (dashed curve), and visible dimension as calculated by Eqs. (2) and (7) (solid curve).
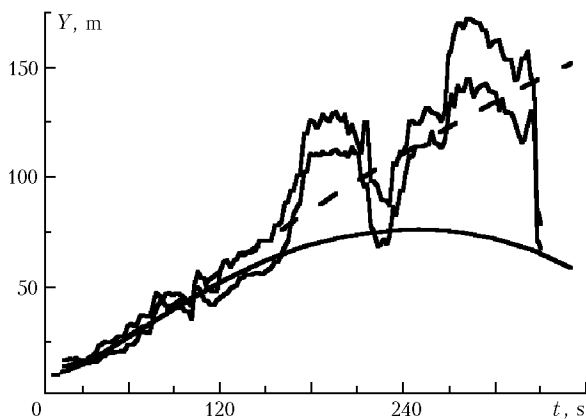


**Fig. 5.** Time dependence of the horizontal cloud dimension in the direction across the wind: result of experimental data processing at division of the integration domain into 27 and 1000 parts (irregular curves), calculation by Eq. (6) (dashed curve), and visible dimension as calculated by Eqs. (5) and (12) (solid curve).
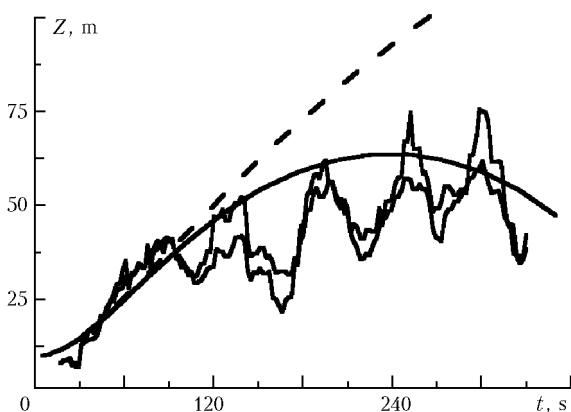


**Fig. 6.** Time dependence of the vertical cloud dimension: result of experimental data processing at division of the integration domain into 27 and 1000 parts (irregular curves), calculation by Eq. (5) (dashed curve), and visible dimension as calculated by Eqs. (5) and (12) (solid curve).

The relatively small discrepancies between the experimental curves are indicative of the sufficient accuracy of spatial integration when calculating cloud dimensions from the experimental data. The excess of the experimental cross cloud dimensions over the calculated ones (see Fig. 5) can be assumingly attributed to fluctuations of the wind direction, which blurred lidar data in the cross direction. In general, the calculated and experimental results are in a good agreement.

## Conclusion

The experiment showed that, using a lidar, one can monitor the concentration distribution in a cloud formed by a pulsed source in real time and with high temporal and spatial resolution. To determine reliably the cloud size and the mass of the substance contained in it, experimental data should be averaged for the time longer than the time of cloud scanning. The latter should be shorter than the characteristic time of change of the cloud dimensions. Numerical simulation was conducted within the framework of the Gauss statistical model. It was demonstrated that the finite sensitivity of the device should necessarily be taken into account when calculating the observed cloud mass and dimensions. The calculated time dependence of the observed cloud dimensions is in a good agreement with the experimental data.

## Acknowledgments

## References

1. P.M. Mushenko, Trudy LGMI, Issue 15, 153$160 (1963).
2. L.N. Krasnovskaya, Tr. Ins. Exp. Meteorol., Issue 27, 76$82 (1972).
3. F.A. Gifford, J. Meteorol. **14**, No. 5, 410$414 (1957).
4. P.V. Nicola, J. Appl. Meteorol. **10**, 962$973 (1971).
5. E.D. Hinkley, ed., *Laser Monitoring of the Atmosphere* (Springer-Verlag, New York, 1976).
6. N.L. Byzova, E.K. Garger, and V.N. Ivanov, *Experimental Studies of Atmospheric Diffusion and Calculations of Admixture Spreading* (Gidrometeoizdat, Leningrad, 1991), 297 pp.

7. F.T.M. Nieuwstadt and Han van Dop, eds., *Atmospheric Turbulence and Air Pollution Modelling* (D. Reidel Publishing Company, 1982).

8. A.S. Monin and A.M. Yaglom, *Statistical Fluid Mechanics: Mechanics of Turbulence* (The MIT press, 1981).

9. E.A. Novikov, Zh. Eksp. Teor. Fiz. **44**, No. 6, 2159$2168 (1963).

10. D. Iordanov, Izv. Akad. Nauk SSSR, Fiz. Atmos. Okeana **13**, No. 7, 781$783 (1977).

11. *Atmosphere. Reference Book* (Gidrometeoizdat, Leningrad, 1991), 509 pp.

12. V.E. Zuev, B.V. Kaul', I.V. Samokhvalov, K.I. Kirkov, and V.I. Tsanev, *Laser Sensing of Industrial Aerosols* (Nauka, Novosibirsk, 1986), 188 pp.

13. Yu.S. Balin and I.A. Razenkov, Atmos. Oceanic Opt. **6**, No. 2, 104$114 (1993).

14. A.Ya. Bogushevich, Atmos. Oceanic Opt. **12**, No. 2, 170$174 (1999).